AMERICAN SOCIETY FOR MICROBIOLOGY | Infection and Immunity

The Type III Secretion System Effector SeoC of *Salmonella enterica* subsp. *salamae* and *S. enterica* subsp. *arizonae* ADP-Ribosylates Src and Inhibits Opsonophagocytosis

Dominic J. Pollard,[a] Joanna C. Young,[a] Valentina Covarelli,[a] Silvia Herrera-León,[b] Thomas R. Connor,[c] Maria Fookes,[c] Danielle Walker,[c] Aurora Echeita,[b] Nicholas R. Thomson,[c,d] Cedric N. Berger,[a] Gad Frankel[a]

MRC Centre for Molecular Bacteriology and Infection, Department of Life Sciences, Imperial College, London, United Kingdom[a]; Sección de Enterobacterias, Servicio de Bacteriología, Centro Nacional de Microbiología, ISCIII, Majadahonda, Spain[b]; Wellcome Trust Sanger Institute, Hinxton, Cambridge, United Kingdom[c]; The London School of Hygiene and Tropical Medicine, London, United Kingdom[d]

***Salmonella* species utilize type III secretion systems (T3SSs) to translocate effectors into the cytosol of mammalian host cells, subverting cell signaling and facilitating the onset of gastroenteritis. In this study, we compared a draft genome assembly of *Salmonella enterica* subsp. *salamae* strain 3588/07 against the genomes of *S. enterica* subsp. *enterica* serovar Typhimurium strain LT2 and *Salmonella bongori* strain 12419. *S. enterica* subsp. *salamae* encodes the *Salmonella* pathogenicity island 1 (SPI-1), SPI-2, and the locus of enterocyte effacement (LEE) T3SSs. Though several key *S.* Typhimurium effector genes are missing (e.g., *avrA*, *sopB*, and *sseL*), *S. enterica* subsp. *salamae* invades HeLa cells and contains homologues of *S. bongori sboK* and *sboC*, which we named *seoC*. SboC and SeoC are homologues of EspJ from enteropathogenic and enterohemorrhagic *Escherichia coli* (EPEC and EHEC, respectively), which inhibit Src kinase-dependent phagocytosis by ADP-ribosylation. By screening 73 clinical and environmental *Salmonella* isolates, we identified EspJ homologues in *S. bongori*, *S. enterica* subsp. *salamae*, and *Salmonella enterica* subsp. *arizonae*. The β-lactamase TEM-1 reporter system showed that SeoC is translocated by the SPI-1 T3SS. All the *Salmonella* SeoC/SboC homologues ADP-ribosylate Src E310 *in vitro*. Ectopic expression of SeoC/SboC inhibited phagocytosis of IgG-opsonized beads into Cos-7 cells stably expressing green fluorescent protein (GFP)-FcγRIIa. Concurrently, *S. enterica* subsp. *salamae* infection of J774.A1 macrophages inhibited phagocytosis of beads, in a *seoC*-dependent manner. These results show that *S. bongori*, *S. enterica* subsp. *salamae*, and *S. enterica* subsp. *arizonae* share features of the infection strategy of extracellular pathogens EPEC and EHEC and shed light on the complexities of the T3SS effector repertoires of *Enterobacteriaceae*.**

Salmonella strains comprise a large group of foodborne bacterial pathogens of the gastrointestinal tract. Originally, the genus *Salmonella* was divided into seven subspecies (I, II, IIIa, IIIb, IV, V, and VI [1]) but is currently classified as two species, *Salmonella bongori*, previously subspecies V, and *Salmonella enterica*. The remaining subspecies have been renamed under the *S. enterica* species as *enterica* (I), *salamae* (II), *arizonae* (IIIa), *diarizonae* (IIIb), *houtenae* (IV), and *indica* (VI), which are further divided into over 2,600 serovars based on their O (oligosaccharide) and H (flagellar) antigens (2).

It is estimated that salmonellosis, the disease caused by consumption of contaminated food and water, is responsible for approximately 1.2 million cases and 450 fatalities per annum in the United States alone (3). Reservoirs of *Salmonella* spp. can be found in a range of domestic and wild animals, such as cattle, swine, poultry, and birds (4). In addition, exposure to exotic reptiles has been increasingly reported as a source of infection due to their growing popularity as pets (5). Salmonellae can cause a variety of conditions aside from the local diarrheal disease, including bacteremia, osteomyelitis, and enterocolitis (6).

The majority of salmonellosis cases observed in mammals and birds are a result of infections with *S. enterica* subsp. *enterica*. As a result, research into the remaining five *S. enterica* subspecies and *S. bongori*, often considered nonpathogenic commensals of cold-blooded vertebrates, is limited to date. Nevertheless, these other salmonellae do cause sporadic disease in mammals, with children and immunocompromised individuals most at risk (7–9). Several fatalities have been reported, and clinical evidence suggests that as a proportion of cases, those infections caused by non-*enterica* (I) subspecies are more likely to cause invasive extraintestinal disease (10).

Salmonellae encode two virulence-associated type III secretion systems (T3SSs) on *Salmonella* pathogenicity island 1 (SPI-1) and SPI-2, which are required for different stages of salmonellosis. T3SSs are macromolecular syringes, which translocate effectors into the membrane and cytosol of cells lining the gastrointestinal mucosae. The SPI-1 T3SS and its effectors are required for the initial infection process involving the invasion of nonphagocytic cell epithelium and M-cells and the stimulation of diarrhea (reviewed in reference 11). Once internalized, the bacterium resides

Received 12 August 2016 **Returned for modification** 12 September 2016 **Accepted** 2 October 2016

Accepted manuscript posted online 10 October 2016

Citation Pollard DJ, Young JC, Covarelli V, Herrera-León S, Connor TR, Fookes M, Walker D, Echeita A, Thomson NR, Berger CN, Frankel G. 2016. The type III secretion system effector SeoC of *Salmonella enterica* subsp. *salamae* and *S. enterica* subsp. *arizonae* ADP-ribosylates Src and inhibits opsonophagocytosis. Infect Immun 84:3618–3628. doi:10.1128/IAI.00704-16.

Editor: V. B. Young, University of Michigan

Address correspondence to Gad Frankel, g.frankel@imperial.ac.uk.

Supplemental material for this article may be found at http://dx.doi.org/10.1128/IAI.00704-16.

within the specialized *Salmonella*-containing vacuole (SCV), where the SPI-2 is utilized for bacterial replication and systemic spreading of the infection. Recent reports have shown that *Salmonella enterica* subsp. *salamae* strains 1582 (serotype 58:d:z6), 1583 (serotype 47:b:1,5) (12), S1635, and S1296 (serovar Sofia, serotype 1,4,12,27:b:−) (13) carry genes similar to those carried by the locus of enterocyte effacement (LEE) pathogenicity island of the human pathogens enteropathogenic and enterohemorrhagic *Escherichia coli* (EPEC and EHEC, respectively) and the mouse pathogen *Citrobacter rodentium*, including the T3SS. Unlike members of *S. enterica*, *S. bongori* lacks SPI-2 and its SPI-1 locus appears to have acquired 11 genes not found in *S. enterica* subsp. *enterica*, 10 of which are homologues of T3SS effectors from EPEC and EHEC (14). For example, SboH from *S. bongori* shares sequential and functional homology to the antiapoptotic effector NleH1 (15). Furthermore, SboC shares 57% sequence identity to the EPEC antiphagocytic effector EspJ (14).

EPEC EspJ is able to ADP-ribosylate the kinase domain of Src, preventing the phosphorylation of the Fcγ-receptor-IIa (FcγRIIa) required for opsonophagocytosis (16, 17), and was the first example of a bacterial ADP-ribosyltransferase (ART) to target a mammalian tyrosine kinase. Mass spectrometry suggested a novel mechanism with coupled amidation and ADP-ribosylation of Src E310, a residue highly conserved throughout the kinase superfamily (18).

While producing a draft genome sequence for *S. enterica* subsp. *salamae* strain 3588/07, we found an *espJ/sboC* homologue, which we named SeoC, within a complex effector protein repertoire. The aim of this study was to determine the prevalence of *espJ/sboC/seoC* in representative clinical and environmental isolates from each of the *S. enterica* subspecies and to characterize their activity in relation to EspJ from EPEC, EHEC, and *C. rodentium*.

MATERIALS AND METHODS

Determination of the effector repertoire of *S. enterica* subsp. *salamae* strain 3588/07. The whole genome of *S. enterica* subsp. *salamae* strain 3588/07 was sequenced using paired-end 454 FLX pyrosequencing using the Titanium chemistry from both 3-kb and 20-kb insert libraries. The read data were assembled using the 454/Roche Newbler assembly program into 138 contigs (N_{50} contig size, 173,757 bp; N_{50} scaffold size, 5,041,913 bp) representing 5,116,235 bp of sequence from 631,936 sequence reads representing 25× total coverage. We compared a draft assembly of *S. enterica* subsp. *salamae* (PATRIC accession no. GCA_000308035.1) against the genomes of *S. enterica* subsp. *enterica* serovar Typhimurium LT2 and *S. bongori* 12419. We performed all-against-all BLAST searches comparing each of these genomes against the *S. enterica* subsp. *salamae* assembly to identify regions with shared sequence similarity. We then visualized the BLAST searches using the Artemis Comparison Tool (19) and used known effectors in the *Salmonella enterica* serovar Typhimurium and *S. bongori* genomes to identify putative coding sequences for effectors in the *S. enterica* subsp. *salamae* assembly. We verified their presence based on a combination of direct examination of the nucleotide or amino acid sequence similarity and identification of their presence along with the same up- and/or downstream genes present in *S.* Typhimurium or *S. bongori*.

Bacterial strains and growth conditions. Bacterial strains used in this study can be found in Tables S1 and S2 in the supplemental material. Bacteria were routinely cultured in Luria-Bertani (LB) broth at 37°C, with tetracycline (6 μg/ml), ampicillin (100 μg/ml), or kanamycin (50 μg/ml) as appropriate.

Seventy-three strains were selected from the Collection of the Spanish National Laboratory for Salmonella. All the *S. enterica* strains were isolated in Spain, while *S. bongori* strains were from the National Salmonella Reference Laboratory at the Centers for Disease Control and Prevention, Atlanta, GA (see Table S2 in the supplemental material).

Construction of *S. enterica* subsp. *salamae* mutants. *S. enterica* subsp. *salamae* mutants (see Table S1 in the supplemental material) were created using the lambda red recombinase method (20). For *S. enterica* subsp. *salamae* Δ*seoC*, a PCR product was generated from *S. enterica* subsp. *salamae* including *seoC* and 500-bp flanking regions using primer pair 15 (see Table S3) and inserted into pGEMT vector by blunt-ended ligation. Inverse PCR with primer pair 16 was used to remove *seoC* coding sequence from this plasmid, and the kanamycin resistance cassette amplified from pKD4 using primer pair 18 was blunt-end ligated into the pGEMT backbone containing the *seoC* flanking regions. Primer pair 15 was used to amplify the kanamycin resistance cassette flanked by 500-bp flanking regions of *seoC*. For *S. enterica* subsp. *salamae* Δ*escN*/Δ*invA*/Δ*ssav* mutants, the kanamycin resistance cassette from pKD4 was amplified with 50-bp flanking regions of *escN*, *invA*, or *ssaV* on either side, using primer pairs 20/21/22. PCR products from the two above methods were transformed by electroporation into electrocompetent *S. enterica* subsp. *salamae* 3558/07 expressing the lambda red genes from an arabinose-inducible promoter within the pKD46 plasmid (20). Clones were selected on 50-μg/ml kanamycin LB agar, cured by growth at 42°C, and verified by PCR and DNA sequencing using primer pairs 17/23/24/25 (for Δ*seoC*/Δ*escN*/Δ*invA*/Δ*ssav*, respectively), 560 bp flanking the *seoC* gene, and primers for the kanamycin cassette.

Plasmid construction. Oligonucleotides for gene amplification and site-directed mutagenesis are shown in Table S3 in the supplemental material, plasmids are shown in Table S4, and the strains from which genes were amplified are shown in Table S1. Briefly, oligonucleotides were used to amplify the gene insert from genomic DNA, and products were purified using the Qiagen PCR purification kit according to the manufacturer's instructions. Target vectors and PCR products were digested for 1 h at 37°C with restriction enzymes before dephosphorylating the cut vector with calf intestinal phosphatase (New England BioLabs [NEB]) for 30 min at 37°C. Inserts and vectors were incubated together at a 3:1 molar ratio for 20 min at room temperature (RT) with T4 DNA ligase (NEB) before transformation into Top10 competent cells. Inserts were confirmed by colony PCR followed by DNA sequencing. Subcloning with EcoRI and HindIII restriction enzymes was used to "cut and paste" EPEC EspJ from pRK5-myc-$EspJ_{EPEC}$ to pMALXE-$EspJ_{EPEC}$. Site-directed mutagenesis was performed either by nonoverlapping inverse PCR followed by blunt-ended ligation or by overlapping inverse PCR and transformation using the QuikChange II site-directed mutagenesis kit (Agilent) according to the manufacturer's instructions.

Screening and sequencing *seoC/sboC/espJ* orthologues among *Salmonella* isolates. PCR was performed using *espJ* primers (primer pair 1 [see Table S3 in the supplemental material]) on bacterial boilates using a PuReTaq-Ready-To-Go PCR bead system (GE Healthcare). The amplification products of *espJ* were purified and sequenced using the same primers. Sequencing was performed on an ABI Prism 3730XL DNA analyzer (Applied Biosystems, Applera Hispania, S.A., Spain) using the *Taq* Dye Deoxy Terminator cycle sequencing kit (Applied Biosystems/Perkin-Elmer). Sequences analysis was performed with Lasergene v.5.0 software (DNAStar, Madison, WI, USA).

Eukaryotic cell maintenance. Cos-7, J774.A1, and HEK293 cells were maintained in Dulbecco's modified Eagle's medium (DMEM; Sigma-Aldrich) containing 4,500 mg/liter glucose supplemented with 10% (vol/vol) heat-inactivated fetal calf serum and 1% (vol/vol) GlutaMAX (Life Technologies) at 37°C and 5% CO_2. HeLa cells were similarly maintained, only with 1,000 mg/liter glucose. Green fluorescent protein (GFP)-FcγIIa-stably transduced Cos-7 cells had the addition of 0.1 μg/ml of puromycin.

Translocation assay. The β-lactamase (TEM-1) translocation assay was performed as previously described (14). Briefly, 8×10^3 HeLa/4×10^3 J774.A1 cells were seeded per well of a 96-well plate (BD Falcon; catalogue no. 353948) 48 h prior to infection. Overnight cultures of *S. enterica* subsp. *salamae* strains were diluted 1:33 and grown for 2 h at 37°C with shaking before inducing TEM fusion expression from pCX340 (21) with 0.05 mM isopropyl-β-D-1-thiogalactopyranoside (IPTG). Cultures were then incubated to an optical density at 600 nm (OD_{600}) of 1.8 (typically a further 30 min) and used to infect monolayers with a multiplicity of infection (MOI) of 100 for 1 h at 37°C, 5% CO_2. The cell monolayers were washed with 100 μl Hanks' buffered salt solution (Gibco), supplemented with 20 mM HEPES and 3 mM probenecid (Sigma), pH 7.4, and developed as described previously (14). Fluorescence emission at 450 nm and 520 nm was measured using a FLUOstar Optima plate reader (excitation wavelength, 410 nm; 10-nm band-pass). The translocation rate was calculated as recommended in the Live Blazer FRET-B/G loading kit manual. Expression of the TEM-1 fusion proteins was analyzed by Western blotting using a mouse anti-β-lactamase antibody (QED Bioscience Inc.; data not shown).

Protein overexpression. EspJ homologues were cloned into pMALX(E) (22) backbone and Src 250–$533_{K295M/Y416F}$ ($Src_{250-533KY}$) and Src 250–$533_{K295M/Y416F/E310A}$ ($Src_{250-533KYE}$) were cloned into pGEX-KG to produce an N-terminally maltose binding protein (MBP)-tagged fusion and N-terminally glutathione *S*-transferase (GST)-tagged fusions, respectively. These vectors were transformed into BL21-STAR competent cells (Novagen), and overnight cultures were used to inoculate 1:100 of fresh LB broth. After growth to an OD_{600} of 0.6 at 37°C, protein expression from the T7 promoter was induced with 1 mM IPTG at 18°C overnight. Cells harvested at 4,500 relative centrifugal force (RCF) were resuspended in MBP lysis buffer (500 mM NaCl, 50 mM *N*-cyclohexyl-3-aminopropanesulfonic acid [CAPS], 5 mM dithiothreitol [DTT], 10% glycerol, pH 11) or GST lysis buffer (300 mM NaCl, 50 mM Na_2HPO_4, 5 mM DTT, 5% glycerol, pH 7.4) before cell disruption by sonication and clarification at 40,000 RCF.

GST-Src 250–533 purifications. Lysis supernatant was passed over a GSTrap 4B Sepharose column (GE Healthcare) to bind GST fusion proteins, and nonspecific interaction mixtures were washed with a 20× column volume of GST lysis buffer before being eluted with 20 mM reduced glutathione-containing elution buffer. Next, gel filtration in lysis buffer using a Superdex 200 10/300 gel filtration column (Invitrogen) was utilized to remove protein aggregates.

***In vitro* ADP-ribosylation assay.** Five hundred microliters of lysis supernatant was incubated with 50 μl of amylose resin (Novagen) for 1 h at 4°C with rotation. After washing 3 times with MBP lysis buffer, 4 μg of GST-tagged $Src_{250-533KY}$ or $Src_{250-533KYE}$ and 10 μM 6-biotin-17-NAD^+ (AMSBio) in phosphate-buffered saline (PBS), pH 7.4, were added. After 1 h, room-temperature (RT) Laemmli buffer was added and samples were boiled to stop the reaction.

Western immunoblotting. After separation by SDS-PAGE, the Bio-Rad Transblot semidry transfer cell was used to transfer samples to a polyvinylidene difluoride (PVDF) membrane for 1 h at 15 V. Membranes were blocked for 1 h at RT with 5% skim milk–PBS-Tween (PBST) (Sigma-Aldrich) before sequential incubation with primary and secondary antibodies in 1% skim milk-PBST for 1 h each with washing in between (see Table S5 in the supplemental material).

Construction of a stably transduced Cos-7 GFP-FcγRIIa cell line. GFP-FcγRIIa was cloned from pEGFP-FcγRIIa (23) into pMXs-IP (Invitrogen). HEK293 cells were seeded in a 6-well plate (Becton Dickinson) at 4.8 × 10^4 cells per well 24 h before transfection. Cells were transfected with 500 ng pMX-IP–GFP-FcγRIIa, 400 ng of Moloney murine leukemia virus (MMLV) plasmid, and 100 ng of vesicular stomatitis virus G protein (VSV-G) plasmid using Lipofectamine (Invitrogen) according to the manufacturer's protocol. After 24 h, transfected cells were washed and fresh medium was added, allowing the cells to produce virions for a further 24 h when the GFP-FcγRIIa packaged virion-containing supernatant was collected. HEPES buffer was added to a final concentration of 20 mM, and the supernatant was filtered through a non-PVDF membrane before being added to a 70 to 90% confluent T25 flask of Cos-7 cells. After 24 h, the transduction of GFP-FcγRIIa was confirmed by fluorescence microscopy. Transduced cells were selected with 0.3 μg/ml puromycin for 1 week before fluorescence-activated cell sorting (FACS) using a BD FACS Aria III cell sorter and assessed using a BD FACS Fortessa III cell analyzer.

Transfection of Cos-7 GFP-FcγRIIa cells. Glass coverslips in 24-well tissue culture plates (Becton Dickinson) were seeded with 5 × 10^4 cells per well 24 h prior to transfection. Cells were transfected using Genejuice transfection reagent (Novagen) at a 3:1 Genejuice/DNA ratio according to the manufacturer's instructions. DNA at 0.5 μg/well was transfected for 14 to 16 h before subjection to the opsonophagocytosis protocol.

***S. enterica* subsp. *salamae* infection of J774.A1/HeLa cells.** J774.A1/HeLa cells were seeded on glass coverslips in a 24-well plate at 1.5 × 10^5/7.5 × 10^4 cells per well 24 h before infection, respectively. Overnight *S. enterica* subsp. *salamae* cultures were diluted 1:33 in Lennox-LB broth and incubated for 2.5 h at 37°C with shaking for 2.5 h to an OD_{600} of 0.8 before infection of macrophages with an MOI of 100. For complementation, genes were expressed from the pWSK29 backbone (24) using 0.05 mM IPTG 30 min prior to and during the infection. After 30 min of infection, bacterium-containing medium was removed and infected cells were challenged with opsonized beads as described below. For assessment of the bacterial invasion/internalization, *S. enterica* subsp. *salamae* expressing GFP from the pFPV25.1 plasmid (25) was used for infection. External bacteria were stained prepermeabilization using the BacTrace goat anti-CSA-1 antibody (Kirkegaard & Perry Laboratories [KPL]).

Gentamicin protection invasion assay. HeLa cells were infected as described above, washed with PBS after 60 min, and incubated with gentamicin-containing medium (200 μg/ml) for a further 60 min. Cells were then washed 5 times with PBS and lysed with 0.1% Triton X-100 before being plated in serial dilutions on LB agar to assess the number of CFU. Internalization is expressed as a percentage of the calculated inoculum.

LDH release cytotoxicity assay. J774.A1 cells were infected as described above, taking supernatant samples at 30 and 60 min. After centrifugation at 4,000 RCF followed by 20,000 RCF to remove mammalian and bacterial cells, supernatants were assessed for lactate dehydrogenase (LDH) release using the CytoTox 96 nonradioactive cytotoxicity assay (Promega) according to the manufacturer's protocol. Absorbance at 490 nm was measured using a medium-only control to calculate the net absorbance, and readings were normalized to uninfected controls.

Bead opsonization and opsonophagocytosis assay. Transfected cells were incubated for 2 h with serum-free DMEM (SF-DMEM). Meanwhile, 3.4-μm Sphero bovine serum albumin (BSA)-coated polystyrene beads (Spherotech) were opsonized for phagocytosis. Per coverslip, 10 μl (Cos-7 GFP-FcγRIIa cells) or 2.5 μl (J774.A1 cells) of bead slurry was washed in 1 ml of 20 mM 2-(*N*-morpholino)ethanesulfonic acid (MES)-8 mM HEPES before incubation with rotation with mouse anti-BSA primary antibody at room temperature (RT). After 1 h, opsonized beads were harvested and resuspended in 1 ml SF-DMEM (Cos-7 GFP-FcγRIIa cells) or serum-containing DMEM (J774.A1 cells) per coverslip before addition to transfected/infected cells. Beads were centrifuged onto the cells at 500 RCF for 5 min. Transfected cells were incubated at 4°C for 15 min before bead-containing medium was replaced with serum-containing DMEM, and phagocytosis was allowed to occur for 90 min. Infected macrophages were incubated with beads for 30 min at 37°C with 5% CO_2. Infected/transfected cells were then washed once with cold tissue-grade PBS on ice before a 7-min staining of extracellular beads using donkey anti-mouse Alexa 488/RRX antibody on 0.2% BSA-PBS before washing twice with PBS and fixation with 3.7% paraformaldehyde (PFA)-PBS for 25 min.

Immunofluorescence staining. Fixed cells were neutralized with 50 mM NH_4Cl-PBS for 15 min and permeabilized with 0.2% Triton X-100–PBS for 2 min. Nonspecific binding was blocked using 0.2% bovine serum albumin (BSA)-PBS for 15 min prior to incubation with primary antibodies (see Table S5 in the supplemental material). After 45 min, cells were

TABLE 1 Comparison of *Salmonella* T3SS effectors[a]

Secretion system or gene	Genomic location	Secreting system(s)	Presence or absence of T3SS effector system or protein in *Salmonella* strain[b]: *S. enterica* subsp. *salamae* 3588/07	*S. enterica* subsp. *salamae* 1582	*S. enterica* subsp. *salamae* 1583	*S. enterica* subsp. *arizonae* CDC346-86	*S. bongori* 12419	*S.* Typhimurium LT2
Secretion systems								
SPI-1 T3SS			+	+	+	+	+	+
SPI-2 T3SS			+	+	+	+	−	+
Gene name								
avrA	SPI-1	SPI-1	−	−	−	−	+	+
sboC/seoC	ROD	SPI-1	+	+	+	+	+	−
sipA (*sspA*)	SPI-1	SPI-1	+	+	+	+	+	+
sipB (*sspB*)	SPI-1	SPI-1	+	+	+	+	+	+
sipC (*sspC*)	SPI-1	SPI-1	+	+	+	+	+	+
sopA	BB	SPI-1	+	4	5	−	−	+
sopD	BB	SPI-1	+	+	+	+	+	+
sopE	fSopE, fSE12	SPI-1	+	?	?	−	−	−
sopE2	BB	SPI-1	+	+	+	+	+	+
sptP	SPI-1	SPI-1	+	+	+	+Ψ	+Ψ	+
sopB (*sigD*)	SPI-5	SPI-1	F	?	?	+	+	+
slrP	BB	SPI-1 and -2	−	−	−	+	+	+
sspHI	ROD	SPI-1 and -2	+	?	?	−	−	+@
gogB	fGifsy-1	SPI-2	−	−	−	−	−	+
pipB	SPI-5	SPI-2	−	−	−	−	−	+
spvB	pSLT plasmid	SPI-2	−	−	−	+	−	+
sseI (*srfH*)	fGifsy-2	SPI-2	−	−	−	+	−	+
sseK1	ROD	SPI-2	−	?	?	+	−	+
sseL	BB	SPI-2	−	?	?	+	−	+
sspH2	SPI-12	SPI-2	−	−	−	+	−	+
pipB2	ROD	SPI-2	+	+	+	−	−	+
sifA	BB	SPI-2	+	+	+	+	−	+
sifB	BB	SPI-2	+	+	+	+	−	+
sopD2	BB	SPI-2	+	+	?	+	−	+
spiC (*ssaB*)	SPI-2	SPI-2	+	+	+	+	−	+
sseF	SPI-2	SPI-2	+	+	+	+	−	+
sseG	SPI-2	SPI-2	+	+	+	+	−	+
sseJ	BB	SPI-2	+	+	+	+	−	+
sseK2	ROD	SPI-2	+	?	?	−	−	+
steA	BB	SPI-2	+	?	?	−	−	+
steB	BB	SPI-2	+	?	?	−	−	+
steC	BB	SPI-2	+	?	?	−	−	+
sseK3	fSE20	−	−	?	?	−	−	−&
sboA	fSB100	*S. bongori* T3SS	−	?	?	−	+	−
sboB	ROD	*S. bongori* T3SS	−	?	?	−	+	−
sboD	ROD	*S. bongori* T3SS	−	?	?	−	+	−
sboE	Degenerate f	*S. bongori* T3SS	−	?	?	−	+Ψ	−
sboF	fSB100	*S. bongori* T3SS	−	?	?	−	+	−
sboG	fSB101	*S. bongori* T3SS	−	?	?	−	+	−
sboH	BB	*S. bongori* T3SS	−	2	−	−	+	−
sboI	ROD	*S. bongori* T3SS	−	−	−	−	+	−
sboJ	ROD	*S. bongori* T3SS	−	−	−	−	+	−
sboK	ROD	*S. bongori* T3SS	+	−	+	−	+	−
sboL	ROD	*S. bongori* T3SS	−	−	2	−	+	−

[a] Symbols and abbreviations: ?, presence not confirmed in the work of Desai et al. (12); +, present; −, absent; Ψ, pseudogene; BB, chromosomal backbone; ROD, region of difference/genomic island; [@], of limited distribution in *S.* Typhimurium (30); &, carried on phage ST64B of other *S.* Typhimurium strains (23); F, *sopB* was missing in *S. enterica* subsp. *salamae*, but there is a fragment of approximately 180 bp that has 58 to 74% sequence similarity to *sopB* in the same genomic position found in *S. bongori*.
[b] Numbers 2, 4, and 5 indicate the number of loci at which the gene is predicted in the genome.

washed 3 times with PBS before being blocked again and incubated with secondary antibodies.

Quantification of bead internalization. The internalization of beads associated with either transfected GFP-FcγRIIa Cos-7 cells or *S. enterica* subsp. *salamae*-infected J774.A1 cells was counted manually by immunofluorescence microscopy. Transfected cells were detected using chicken anti-myc antibody (Bethyl Laboratories), and bacteria were visualized with BacTrace goat anti-CSA-1 antibody (KPL).

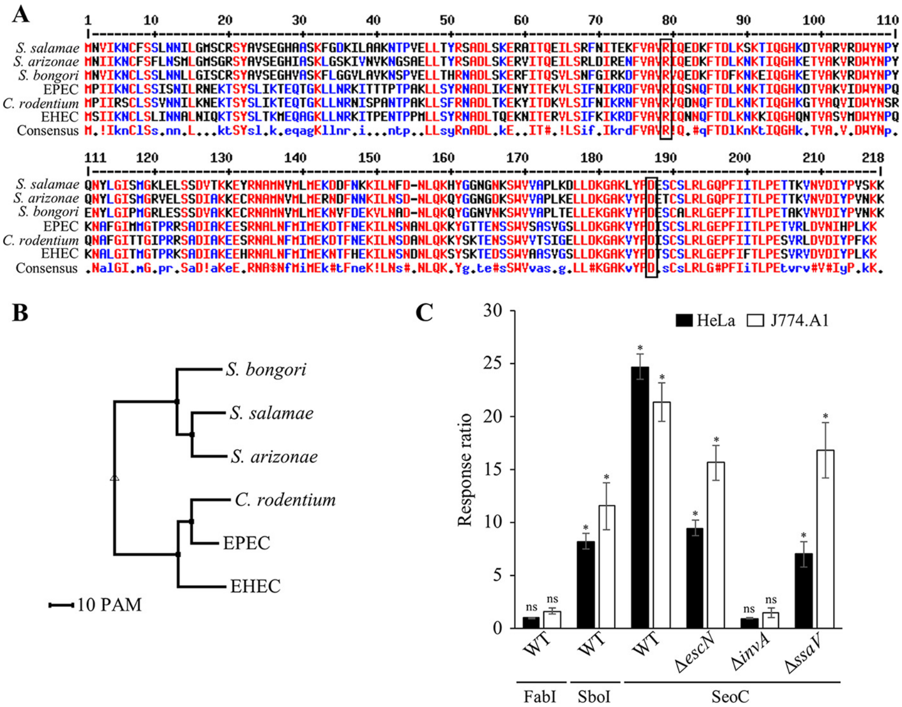

FIG 1 Sequence alignment of EspJ homologues and protein translocation. (A) Sequence alignment of the EspJ homologues with consensus sequence. Residues are colored red for high consensus, blue for low consensus, and black for neutral consensus. The conserved residues R79 and D187 crucial for EPEC EspJ activity are highlighted with a black box. (B) Phylogenetic analysis of the EspJ homologues showing separation of EPEC, EHEC, and *C. rodentium* homologues from the *Salmonella* homologues. A scale for point accepted mutations (PAM) is displayed. (C) *S. enterica* subsp. *salamae* SeoC is translocated via the SPI-1 (Δ*invA*), but not via the SPI-2 (Δ*ssaV*) or LEE (Δ*escN*), T3SS during *S. enterica* subsp. *salamae* infection of HeLa and J774.A1 cells. The T3SS effector SboI and FabI were used as positive and negative controls, respectively. Results are averages from three experiments, each in quadruplicate wells. The error bars represent standard errors of the means. Statistical analyses were performed with GraphPad Prism software using a one-way analysis of variance followed by Bonferroni posttest (*, $P < 0.01$). Asterisks represent significance compared to uninfected cells; ns, not significant.

Accession number(s). The *S. enterica* subsp. *salamae* 3588/07 genome sequencing reads from the 454 platform have been deposited in the Short Read Archive with accession no. ERR043066.

RESULTS

Effector repertoire of *S. enterica* subsp. *salamae* 3588/07. The majority of sequenced *S. enterica* strains are from the *enterica* subspecies, but recently, a few genomes have been annotated from the non-*enterica* subspecies (12, 13, 26). We sequenced the genome of *S. enterica* subsp. *salamae* 3588/07 in order to compare its T3SS effector repertoire to other *Salmonella* strains. Of the seven *S. enterica* subsp. *salamae* isolates, four were from a water bath area which strain 3588/07 was selected to represent. The draft genome sequence is represented by 140 contigs and is 5,116,236 bp in size. In agreement with previously sequenced *S. enterica* subsp. *salamae* strains (12, 13), *S. enterica* subsp. *salamae* 3588/07 carries the SPI-1, SPI-2, and LEE T3SSs, including the signature LEE region proteins encoded by *escN*, the ATPase required for EPEC/EHEC T3SS effector translocation (27), and the translocon proteins EspA/B/D. The EPEC/EHEC outer membrane adhesin intimin was present along with six translocated effectors, including the intimin receptor Tir (28). However, the LEE-encoded effectors Map, EspG, and EspH were missing (29). The entire effector repertoire of *S. enterica* subsp. *salamae* 3588/07 (Table 1) reveals that several key effectors found in *S.* Typhimurium are not present, including the anti-inflammatory effectors AvrA (29) and GogB (30) and the deubiquitinase SseL (31) (Table 1). In particular, only a short, 189-bp fragment of the *sopB* gene, which is considered a core effector with regard to *Salmonella* virulence, is found in the *S. enterica* subsp. *salamae* 3588/07 genome, compared to the 1,686 bp in *S.* Typhimurium. *S. enterica* subsp. *salamae* 3588/07 also encodes the effectors SteA, SteB, SteC, SopE, SspH1, and SseK2, which have not been previously found in *S. enterica* subsp. *salamae* strains (12). In addition, the *S. bongori* effectors SboK and SboC are also present in *S. enterica* subsp. *salamae* 3588/07. SboC is homologous to the EPEC, EHEC, and *C. rodentium* antiphagocytic effector EspJ; we named the *S. enterica* subsp. *salamae* homologue SeoC (*Salmonella enterica* outer protein C).

Prevalence of *sboC*/*seoC* in *S. bongori* and *S. enterica* spp. We investigated the prevalence of *seoC* across the *Salmonella* genus by screening 73 clinical and environmental *Salmonella* isolates by PCR. Strain selection was based upon belonging to different species/subspecies of *Salmonella* and to the most frequent serotypes within each species/subspecies and, if possible, being isolated from human/nonhuman sources (see Table S2 in the supplemental material). All tested *S. bongori* isolates were *sboC* positive. Of the *S. enterica* isolates, *seoC* was found in 4 out of 7 isolates belonging to subspecies *salamae* and in 8 out of 9 isolates belonging to subspecies *arizonae* but not in any isolates of subspecies *enterica*, *diarizonae*, or *houtenae* (see Table S2).

Amino acid sequence alignment (Fig. 1A) revealed that SeoC from *S. enterica* subsp. *arizonae* and that from *S. enterica* subsp. *salamae* share 83% sequence identity and 77%/78% identity, re-

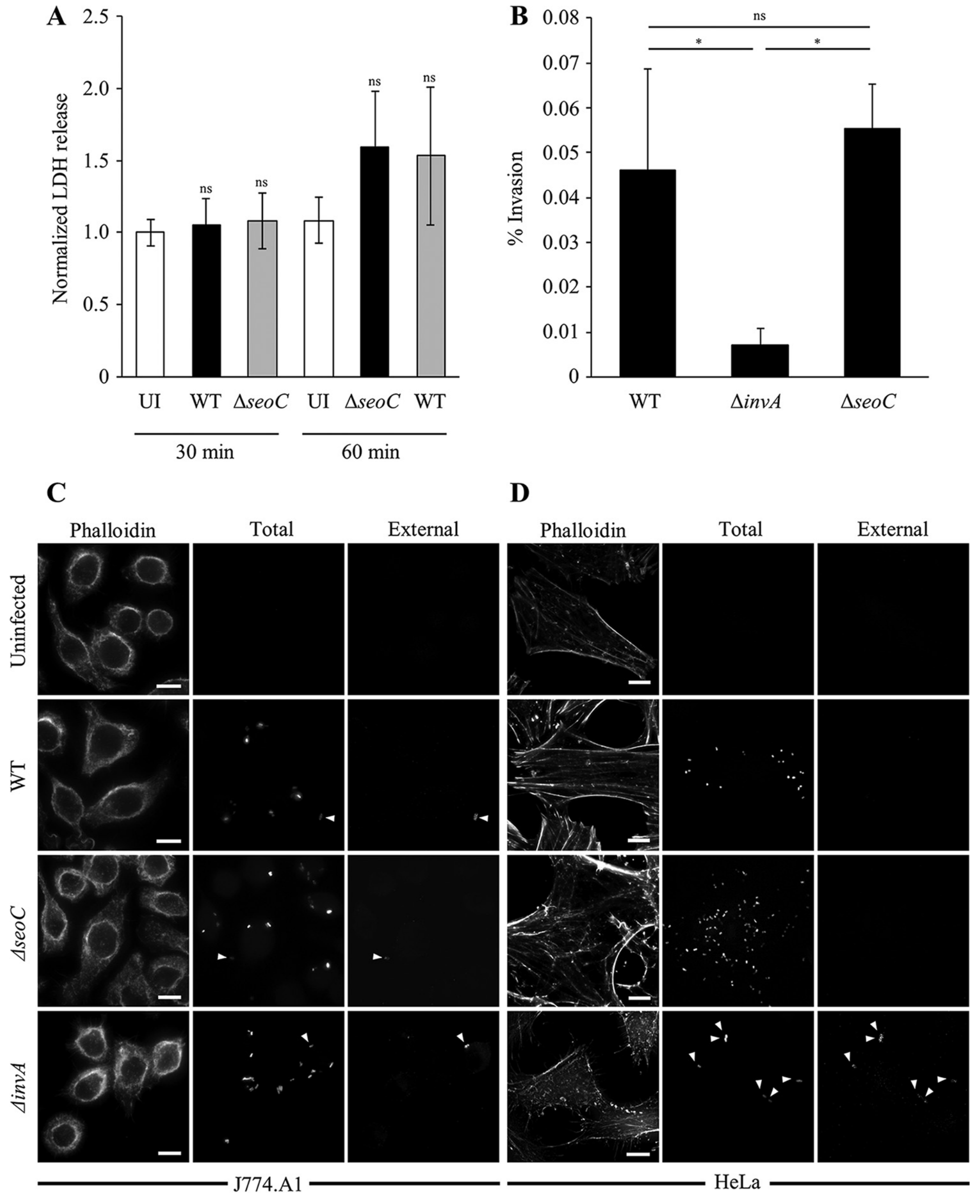

FIG 2 Internalization of *S. enterica* subsp. *salamae* 3588/07 during infection of HeLa and J774.A1 cells. (A) WT and Δ*seoC* *S. enterica* subsp. *salamae* strains do not cause cell lysis compared to uninfected J774.A1 cells 30 or 60 min postinfection. Data represent the averages from three experiments, each in triplicate. UI, uninfected; ns, not significant. (B) Gentamicin protection assay of HeLa cells infected with WT *S. enterica* subsp. *salamae* or Δ*seoC* or Δ*invA* mutant. There was no significant difference between *S. enterica* subsp. *salamae* WT and Δ*seoC* strain invasiveness, while the Δ*invA* strain was significantly less invasive than both WT and Δ*seoC* strains. Results are the mean ± standard error of the mean from three or more independent experiments. Statistical analyses were performed with GraphPad Prism software using a one-way analysis of variance followed by Bonferroni posttest (*, $P < 0.01$; ns, not significant). (C and D) J774.A1 (C) and HeLa (D) cells were infected with WT *S. enterica* subsp. *salamae* or the Δ*seoC* or Δ*invA* mutant expressing GFP. External bacteria were stained with anti-CSA-1 antibody before cell permeabilization. All strains were internalized by J774.A1 macrophages (C). WT and Δ*seoC* strains invaded HeLa cells, while the Δ*invA* strain was not invasive (D). Arrowheads indicate external bacteria. Bars, 10 μm.

spectively, to SboC from *S. bongori*. Between 56% and 58% sequence identity is shared between the *Salmonella* SeoC/SboC and EspJ from EPEC, EPEC, and *C. rodentium* (see Table S6 in the supplemental material). Sequence variation was concentrated at the N-terminal 50 amino acids with only around 35% sequence identity between the *E. coli*/*C. rodentium* and *Salmonella* homologues (see Table S6). Typically, this region harbors a 20- to 30-residue secretion signal, required for specific targeting to the correct secretion system. Phylogenetic analysis revealed that the *Salmonella* and the *E. coli*/*C. rodentium* homologues fall on separate branches in the tree (Fig. 1B). However, residues R79 and D187, required for EPEC EspJ ART activity, are preserved in all EspJ/SeoC homologues, suggesting a conserved catalytic function (Fig. 1A, black box).

***S. enterica* subsp. *salamae* SeoC is translocated by the SPI-1 T3SS.** In order to determine through which T3SS the *S. enterica* subsp. *salamae* SeoC is translocated, translocation assays were performed using wild-type (WT) *S. enterica* subsp. *salamae* and

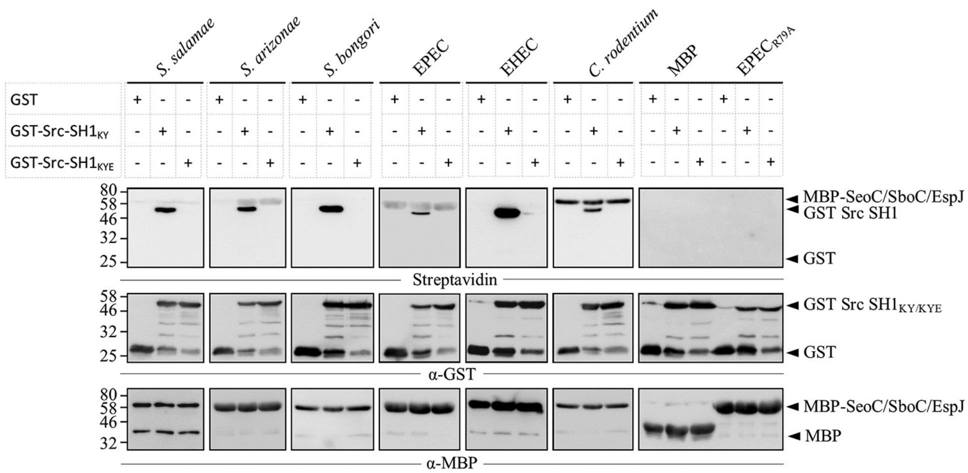

FIG 3 *Salmonella* and *E. coli* EspJ homologues ADP-ribosylate Src E310 *in vitro*. MBP-tagged EspJ homologues bound to amylose resin were incubated with Src-SH1$_{KYE}$ and 6-biotin-17-NAD$^+$ (NAD-biotin) for 1 h and analyzed by Western blotting. ADP-ribosylated proteins were detected using a streptavidin-horseradish peroxidase conjugate (top row), while the anti-GST antibody revealed GST-tagged Src-SH1$_{KY/KYE}$ (middle row) and the anti-MBP antibody revealed MBP-tagged SeoC/SboC/EspJ (bottom row). The proteins detected by Western blotting are indicated with arrowheads on the right. All EspJ homologues were able to ADP-ribosylate GST-Src-SH1$_{KY}$ but not GST-Src-SH1$_{KYE}$. Numbers at left are molecular masses in kilodaltons.

LEE (Δ*escN*), SPI-1 (Δ*invA*), and SPI-2 (Δ*ssaV*) T3SS nonfunctional mutants expressing SeoC fused to the TEM-1 reporter. The housekeeping/cytosolic protein FabI fused to TEM-1, used as a negative control, was not translocated when expressed in WT *S. enterica* subsp. *salamae*, while the *S. bongori* T3SS effector SboI, which was used as a positive control, was translocated into both HeLa cells and J774.A1 macrophages. SeoC-TEM was translocated into both HeLa cells and J774.A1 macrophages following infection with WT *S. enterica* subsp. *salamae*, and to a lesser extent from the Δ*escN* and Δ*ssaV* mutants. In contrast, no translocation was seen from the Δ*invA* strain (Fig. 1C), suggesting that SeoC is an SPI-1 effector.

***S. enterica* subsp. *salamae* invades phagocytic and epithelial cells independently of SeoC.** *S. enterica* subsp. *salamae* is mainly isolated from extraintestinal infections (10). We therefore aimed to investigate the invasion potential of *S. enterica* subsp. *salamae* and any involvement of SeoC in this process, considering that EspJ has an antiphagocytic activity, albeit of opsonized particles (16). *Salmonella* expressing GFP (25) was used to infect HeLa cells and J774.A1 macrophages. Lactate dehydrogenase (LDH) release, indicative of cell lysis, measured 30 and 60 min after infection of J774.A1 with WT and Δ*seoC S. enterica* subsp. *salamae*, revealed no significant increase over uninfected cells (Fig. 2A), suggesting that these strains are not cytotoxic. Gentamicin protection invasion assays showed that while *S. enterica* subsp. *salamae* Δ*invA* was significantly less invasive into HeLa cells, no significant difference was seen between the WT and *S. enterica* subsp. *salamae* Δ*seoC* strains (Fig. 2B). Extracellular bacterial staining, using the anti-CSA-1 antibody prepermeabilization, confirmed that *S. enterica* subsp. *salamae* and *S. enterica* subsp. *salamae* Δ*seoC* invaded both phagocytic and epithelial cells (Fig. 2C and D). The SPI-1 T3SS-deficient Δ*invA* strain was still internalized by J774.A1 macrophages but unable to invade HeLa cells. Together, these data show that, similarly to EspJ, SeoC does not play a role in inhibition of *cis*-phagocytosis (uptake of nonopsonized bacteria).

SeoC ADP-ribosylates Src E310. We have previously reported that EPEC EspJ inhibits Src by ADP-ribosylation of E310 within its protein kinase domain (SH1) (17). In order to determine if SeoC from *S. enterica* subsp. *salamae* and *S. enterica* subsp. *arizonae*, SboC from *S. bongori*, and EspJ from EHEC and *C. rodentium* share this activity, we performed an *in vitro* ADP-ribosylation assay. Purified MBP-tagged effectors and GST-tagged Src-SH1$_{K295M/Y416F}$ (Src-SH1$_{KY}$; K295M, kinase dead; Y416F, autophosphorylation mutant) were incubated with NAD-biotin and then analyzed by Western blotting. This revealed that SeoC, SboC, and EspJ ADP-ribosylated GST-Src-SH1$_{KY}$ (Fig. 3, lower band, streptavidin panel) and also had various levels of autoactivity (Fig. 3, upper band, streptavidin panel). No ADP-ribosylation was detected using the negative control GST or when GST-Src was incubated with MBP-EspJ-EPEC$_{R79A}$ (ART catalytic mutant) or MBP. Importantly, we detected no ADP-ribosylation of Src mutated at residue E310 (Src-SH1$_{KYE}$), suggesting that the target residue is shared between SeoC, SboC, and EspJ.

Ectopic expression of SeoC inhibits FcγRIIa-mediated phagocytosis. Src kinase is involved in the regulation of many cellular processes, including cell proliferation and differentiation, cell motility, and phagocytosis (reviewed in reference 32). Src phosphorylates the cytoplasmic immunotyrosine activation motifs (ITAMs) of FcγRIIa, allowing the recruitment of Syk kinase and initiating the signaling cascade for phagocytic actin remodeling. To assess the inhibition of phagocytosis by the different SeoC/SboC/EspJ homologues, we generated a Cos-7 cell line stably expressing FcγRIIa. The cells were then transfected with the different SeoC/SboC/EspJ homologues before being challenged with IgG-opsonized beads. The internal/external localization of cell-associated beads in transfected cells was observed by immunofluorescence (Fig. 4A). Mock-transfected cells or cells transfected with EPEC EspJ$_{R79A/D187A}$ (ART mutant) were used as negative controls. Immunofluorescence analysis showed that all the SeoC/SboC/EspJ homologues reduced bead internalization from 60% in mock- and EspJ$_{R79A/D187A}$-transfected cells to below 10% (Fig. 4B). Thus, the ADP-ribosylation of Src appears inhibitory, and each effector is capable of inhibiting opsonophagocytosis, independently of other effector proteins.

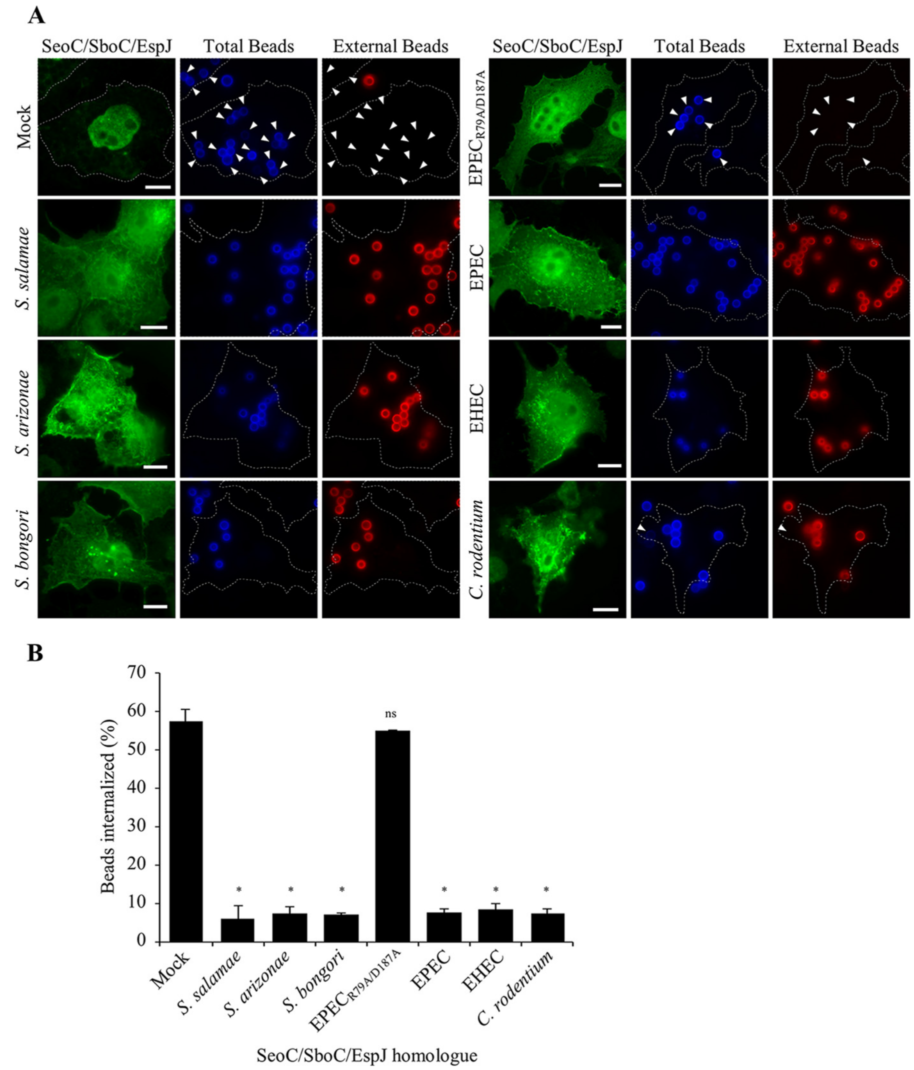

FIG 4 Ectopic expression of *Salmonella* EspJ homologues inhibits FcγRIIa-mediated phagocytosis. Cos-7 cells stably expressing GFP-FcγRIIa and transfected with plasmids encoding Myc-tagged SeoC/SboC/EspJ homologues were challenged with IgG-opsonized 3-μm beads. (A) Staining pre- and postpermeabilization revealed external beads (red), total beads (blue), and SeoC/SboC/EspJ-transfected cells (green). Representative immunofluorescence images of pRK5-SeoC/SboC/EspJ-transfected cells are shown. Arrowheads indicate the internalization of beads in SeoC/SboC/EspJ-transfected cells; dotted lines indicate the cell outlines. Bars, 10 μm. (B) Total/external cell-associated beads were counted for EspJ-transfected cells, revealing inhibition of bead phagocytosis by all SeoC/SboC/EspJ homologues compared to mock-transfected (Mock) or EPEC $EspJ_{R79A/D187A}$ (ART mutant)-transfected cells. Results are the mean ± standard error of the mean from three independent experiments. Statistical analyses were performed with GraphPad Prism software using a one-way analysis of variance followed by Bonferroni posttest (*, $P < 0.01$; ns, not significant).

SeoC inhibits FcγR-mediated phagocytosis during *Salmonella* infection. To confirm the inhibitory activity of SeoC during infection, J774.A1 macrophages were infected with WT *S. enterica* subsp. *salamae*, *S. enterica* subsp. *salamae* Δ*seoC*, and *S. enterica* subsp. *salamae* Δ*seoC* complemented with plasmids carrying *seoC* or $seoC_{R79A}$ and then challenged with IgG-opsonized beads. Immunofluorescence revealed that macrophages infected with WT *S. enterica* subsp. *salamae* displayed reduced phagocytosis of cell-associated beads (<18%) compared to uninfected cells (57%) or cells infected with *S. enterica* subsp. *salamae* Δ*seoC* (68%) (Fig. 5A and B). *S. enterica* subsp. *salamae* Δ*seoC* complemented with *seoC* restored inhibition of phagocytosis (26%), whereas the $seoC_{R79A}$ strain had a level of phagocytosis similar to that of the Δ*seoC* mutant, confirming that ADP-ribosylation activity of SeoC is required for inhibition of phagocytosis.

DISCUSSION

In this study, genomic sequencing revealed the effector repertoire of the SPI-1, SPI-2, and LEE T3SSs of *S. enterica* subsp. *salamae* 3588/07, a crucial determinant for bacterial infection strategies and host specificities. For example, the absence of *sseJ* from *Salmonella enterica* serovar Typhi was linked to reduced cytotoxicity in *in vitro* infection models (33). Similarly, a *Salmonella enterica* serovar Typhimurium *slrP* mutant caused a colonization defect in mice but had no effect in calves (34). Despite its importance in S. Typhimurium, SlrP is not found in *S. enterica* subsp. *salamae* and is observed only as a pseudogene in many other *Salmonella* strains. We observed six effector genes not previously seen in *S. enterica* subsp. *salamae*. These were *steA*, *steB*, and *steC*, with unknown function; *sseK2*, which is similar in sequence to the EPEC/EHEC

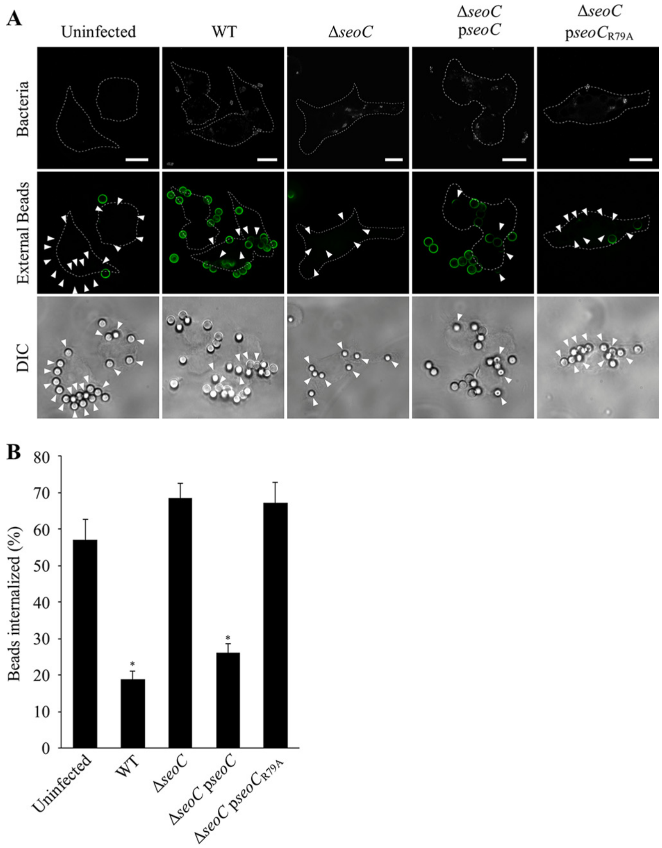

FIG 5 SeoC inhibits FcγRIIa-mediated phagocytosis during *S. enterica* subsp. *salamae* infection of J774.A1 macrophages. J774.A1 macrophages were infected with WT *S. enterica* subsp. *salamae* 3588/07 or Δ*seoC* mutant with or without complementation by pWSK29-SeoC/SeoC$_{R79A}$ (p*seoC*/p*seoC*$_{R79A}$) before challenge with IgG-opsonized beads. (A) Representative immunofluorescence images are shown with external beads stained prepermeabilization (green), total beads shown using differential interference contrast (DIC), and bacteria stained with anti-CSA-1 (white). Macrophage outlines are shown with dotted lines. Arrowheads indicate the internalization of cell-associated beads by infected macrophages. Bar, 10 μm. (B) External and total cell-associated beads were counted, revealing that infection with WT *S. enterica* subsp. *salamae* 3588/07 reduced internalization from 57% of beads for uninfected cells to 18.8%. Deletion of *seoC* removed the inhibition of phagocytosis, while complementation with WT *seoC* but not *seoC*$_{R79A}$ (ART mutant) was able to restore the inhibition. Results are the mean ± standard error of the mean from three independent experiments. Statistical analyses were performed with GraphPad Prism software using a one-way analysis of variance followed by Bonferroni posttest (*, $P < 0.01$).

anti-inflammatory effector NleB (35); the NF-κB inhibitor with E3 ligase activity *sspH1* (36); and the guanine nucleotide exchange factor (GEF) gene *sopE*. In *S.* Typhimurium, a *sopE*, *sopE2*, and *sopB* triple mutant is noninvasive (37). Both *sopE* and *sopE2* are present in *S. enterica* subsp. *salamae* 3558/07, but *sopB*, which contributes to invasion, fluid secretion, SCV development, and intracellular survival (38, 39), and *avrA*, which also supports intracellular survival (29), were absent. Desai et al. identified paralogues of *S. bongori* effector SboH in *S. enterica* subsp. *salamae* 1582, SboK and SboL in *S. enterica* subsp. *salamae* 1583, and SboC in both strains (12). *S. enterica* subsp. *salamae* 3588/07 possesses SboK, which has no known function but is predicted to have a domain organization similar to SlrP, and SboC, the predicted homologue of EPEC/EHEC EspJ. Strain 3588/07 was selected to represent the four of seven *S. enterica* subsp. *salamae* isolates originating from water bath areas. Differences in its effector repertoire from those of other *S. enterica* subsp. *salamae* strains highlight that the remaining six isolates are likely to possess unique subsets of effectors, which could be revealed by further genome sequencing.

PCR screening showed that *sboC/seoC* was present in *S. bongori* (6 from 6), *S. enterica* subsp. *salamae* (4 from 7), and *S. enterica* subsp. *arizonae* (8 from 9) isolates, but none of the *S. enterica* subsp. *diarizonae* and *S. enterica* subsp. *houtenae* isolates tested. *S. bongori* SboC is known to be translocated by the T3SS (14), and this study shows that *S. enterica* subsp. *salamae* SeoC is mainly a substrate of the SPI-1 T3SS. SeoC did, however, inhibit phagocytosis during the infection of murine macrophages, as did the ectopic expression of all tested SeoC/SboC/EspJ homologues within a GFP-FcγRIIa-expressing Cos-7 cell line. It is possible for effector proteins to be substrates of more than one secretion system at different stages of infection, as is the case for SlrP (40). For SeoC, this could explain the reduction in translocation in LEE and SPI-2 T3SS mutant strains, which would be interesting to investigate using secretion assays specific to each T3SS.

Salmonella and *E. coli* are members of the same *Enterobacteriaceae* family with common ancestry over 100 million years ago (41). While pathogenic *E. coli* types such as EPEC and EHEC possess a LEE-encoded T3SS and have adapted an extracellular lifestyle, the majority of *Salmonella* strains have SPI-1 and SPI-2 T3SSs for invasion and intracellular replication, respectively. The SPI-1 T3SS was acquired prior to the divergence of *S. bongori* and *S. enterica*, after which the SPI-2 T3SS was introduced, before separation into further subspecies (42). Pathogenicity islands are generally acquired by horizontal gene transfer but can also be carried in integrative elements such as cryptic prophages (37). Horizontal gene transfer has allowed the diversification and specialization of *Salmonella* infection strategies, and the distribution of the SeoC/SboC/EspJ homologues in *Salmonella* and *E. coli/C. rodentium* is a good example of this.

The presence of both SPI-1 and SPI-2 T3SSs in *S. enterica* subsp. *salamae* and *S. enterica* subsp. *arizonae* suggests an intracellular lifestyle, while the identification of a LEE-encoded T3SS in *S. enterica* subsp. *salamae* could promote the opposite. It has been reported that *S. enterica* subsp. *arizonae* and *S. enterica* subsp. *diarizonae* are internalized poorly by J774.A1 macrophages (43). Additionally, from a variety of *Salmonella* serovars isolated from crocodiles, only subspecies *enterica* and not *salamae* or *diarizonae* displayed invasive phenotypes in a mouse model system (44). In fact, the presence of both SPI-1 and SPI-2 does not necessarily confer invasiveness *in vivo*, as although the transfer of SPI-2 to *S. bongori* increased intracellular persistence in cell culture, systemic pathogenicity in a murine model was not possible (45). We showed that *S. enterica* subsp. *salamae* can invade both J774.A1 and HeLa cells in a SeoC-independent manner and lacks the actin-rich pedestals characteristic of the LEE T3SS. This observation is interesting considering the lack of *sopB* and *avrA* in *S. enterica* subsp. *salamae*, which are key effectors for *S.* Typhimurium invasiveness and intracellular survival. For further characterization of the *salamae* subspecies, it will be useful to investigate invasiveness into other epithelial and macrophage cell lines. The SeoC-independent invasiveness of *S. enterica* subsp. *salamae* shows that SeoC, like EspJ, does not have a role in the inhibition of *cis*-phagocytosis.

Inhibition of phagocytosis by EPEC EspJ is mediated by amidation and ADP-ribosylation of the kinase domain of Src (17). Many bacterial toxins possess ART activity, and several T3SS effector proteins with ART activity have been identified, including *Pseudomonas syringae* HopF2, *Pseudomonas aeruginosa* ExoS and ExoT, and *Salmonella* SpvB. HopF2 shares 20 to 25% sequence identity with the SeoC/SboC/EspJ homologues and ADP-ribosylates multiple mitogen-activated protein kinases (MAPKs) and RIN4, inhibiting plant pathogen-associated molecular pattern (PAMP)-triggered defenses (46, 47). The catalytic activity of SpvB is essential for virulence of *S*. Typhimurium in mice (48), via the modification of actin, a target for many ADP-R toxins, including *Clostridium botulinum* C2, *Clostridium perfringens* iota toxin, and the *Clostridium difficile* toxin (CDT) (49). Of the non-*enterica* subspecies, *spvB* is present only in *S. enterica* subsp. *arizonae*, making SeoC and SboC the first T3SS translocated ARTs identified in *S. enterica* subsp. *salamae* and *S. bongori*. We showed that all the EspJ homologues ADP-ribosylate E310 within the kinase domain of Src, inhibiting Src-dependent phagocytosis signaling. ExoT also inhibits phagocytosis and has many observed targets, including Ras, ezrin/radixin/moesin (ERM) proteins, and Rab5 (50). As Src E310 is highly conserved throughout the kinase superfamily, the SeoC/SboC/EspJ homologues may, too, have additional targets, the discovery of which is vital for uncovering the ultimate role of these effectors. This could be pursued using proteomic mass spectrometry after *Salmonella/E. coli* infections to identify ADP-ribosylated proteins or changes to the phosphoproteome indicating the inactivation of target kinases.

The presence of SeoC/SboC/EspJ homologues in a subset of bacteria with stark differences in their infection strategies displays the importance of horizontal gene transfer for shaping the complex T3SS effector repertoire of *Enterobacteriaceae*. It would be interesting to study the consequences of expressing SeoC/SboC in *S*. Typhimurium, which lacks this translocated enzyme, using the mouse model of salmonellosis. In combination with powerful mass spectrometry analysis, this will help uncover the ultimate impact of these homologues on *Salmonella* infection strategies.

ACKNOWLEDGMENTS

We thank Diana Munera, Ana Arbeloa, Michael Bright, Aurelie Mousnier, and Abigail Clements for their exceptional technical help over several years.

WTSI authors are supported by Wellcome Trust grant number 098051.

FUNDING INFORMATION

This work, including the efforts of Gad Frankel and Cedric Nicolas Berger, was funded by Wellcome Trust. This work, including the efforts of Gad Frankel, Dominic Pollard, Joanna Young, and Valentina Covarelli, was funded by Medical Research Council (MRC).

REFERENCES

1. **Kauffmann F.** 1966. On the history of salmonella research. Zentralbl Bakteriol Orig **201:**44–48. (In German.)
2. **Guibourdenche M, Roggentin P, Mikoleit M, Fields PI, Bockemühl J, Grimont PAD, Weill FX.** 2010. Supplement 2003–2007 (no. 47) to the White-Kauffmann-Le Minor scheme. Res Microbiol **161:**26–29. http://dx.doi.org/10.1016/j.resmic.2009.10.002.
3. **Scallan E, Hoekstra RM, Angulo FJ, Tauxe RV, Widdowson MA, Roy SL, Jones JL, Griffin PM.** 2011. Foodborne illness acquired in the United States—major pathogens. Emerg Infect Dis **17:**7–15. http://dx.doi.org/10.3201/eid1701.P11101.
4. **Rodriguez A, Pangloli P, Richards HA, Mount JR, Draughon FA.** 2006. Prevalence of Salmonella in diverse environmental farm samples. J Food Prot **69:**2576–2580.
5. **Mermin J, Hutwagner L, Vugia D, Shallow S, Daily P, Bender J, Koehler J, Marcus R, Angulo FJ.** 2004. Reptiles, amphibians, and human Salmonella infection: a population-based, case-control study. Clin Infect Dis **38**(Suppl 3)**:**S253–S261. http://dx.doi.org/10.1086/381594.
6. **Gordon MA.** 2011. Invasive nontyphoidal Salmonella disease: epidemiology, pathogenesis and diagnosis. Curr Opin Infect Dis **24:**484–489. http://dx.doi.org/10.1097/QCO.0b013e32834a9980.
7. **Lakew W, Girma A, Triche E.** 2013. Salmonella enterica serotype Arizonae meningitis in a neonate. Case Rep Pediatr **2013:**813495. http://dx.doi.org/10.1155/2013/813495.
8. **Hall ML, Rowe B.** 1992. Salmonella arizonae in the United Kingdom from 1966 to 1990. Epidemiol Infect **108:**59–65. http://dx.doi.org/10.1017/S0950268800049505.
9. **Nair S, Wain J, Connell S, de Pinna E, Peters T.** 2014. Salmonella enterica subspecies II infections in England and Wales—the use of multilocus sequence typing to assist serovar identification. J Med Microbiol **63:**831–834. http://dx.doi.org/10.1099/jmm.0.072702-0.
10. **Abbott SL, Ni FCY, Janda JM.** 2012. Increase in extraintestinal infections caused by Salmonella enterica subspecies II–IV. Emerg Infect Dis **18:**637–639. http://dx.doi.org/10.3201/eid1804.111386.
11. **Wallis TS, Galyov EE.** 2000. Molecular basis of Salmonella-induced enteritis. Mol Microbiol **36:**997–1005. http://dx.doi.org/10.1046/j.1365-2958.2000.01892.x.
12. **Desai PT, Porwollik S, Long F, Cheng P, Wollam A, Clifton SW, Weinstock GM, McClelland M.** 2013. Evolutionary genomics of Salmonella enterica subspecies. mBio **4:**e00579-12. http://dx.doi.org/10.1128/mBio.00579-12.
13. **Chandry PS, Gladman S, Moore SC, Seemann T, Crandall KA, Fegan N.** 2012. A genomic island in Salmonella enterica ssp. salamae provides new insights on the genealogy of the locus of enterocyte effacement. PLoS One **7:**e41615. http://dx.doi.org/10.1371/journal.pone.0041615.
14. **Fookes M, Schroeder GN, Langridge GC, Blondel CJ, Mammina C, Connor TR, Seth-Smith H, Vernikos GS, Robinson KS, Sanders M, Petty NK, Kingsley RA, Bäumler AJ, Nuccio S-P, Contreras I, Santiviago CA, Maskell D, Barrow P, Humphrey T, Nastasi A, Roberts M, Frankel G, Parkhill J, Dougan G, Thomson NR.** 2011. Salmonella bongori provides insights into the evolution of the Salmonellae. PLoS Pathog **7:**e1002191. http://dx.doi.org/10.1371/journal.ppat.1002191.
15. **Hemrajani C, Berger CN, Robinson KS, Marchès O, Mousnier A, Frankel G.** 2010. NleH effectors interact with Bax inhibitor-1 to block apoptosis during enteropathogenic Escherichia coli infection. Proc Natl Acad Sci U S A **107:**3129–3134. http://dx.doi.org/10.1073/pnas.0911609106.
16. **Marchès O, Covarelli V, Dahan S, Cougoule C, Bhatta P, Frankel G, Caron E.** 2008. EspJ of enteropathogenic and enterohaemorrhagic Escherichia coli inhibits opsono-phagocytosis. Cell Microbiol **10:**1104–1115. http://dx.doi.org/10.1111/j.1462-5822.2007.01112.x.
17. **Young JC, Clements A, Lang AE, Garnett JA, Munera D, Arbeloa A, Pearson J, Hartland EL, Matthews SJ, Mousnier A, Barry DJ, Way M, Schlosser A, Aktories K, Frankel G.** 2014. The Escherichia coli effector EspJ blocks Src kinase activity via amidation and ADP ribosylation. Nat Commun **5:**5887. http://dx.doi.org/10.1038/ncomms6887.
18. **Hanks S, Hunter T.** 1995. Protein kinases 6. The eukaryotic protein kinase superfamily: kinase (catalytic) domain structure and classification. FASEB J **9:**576–596.
19. **Carver TJ, Rutherford KM, Berriman M, Rajandream M-A, Barrell BG, Parkhill J.** 2005. ACT: the Artemis Comparison Tool. Bioinformatics **21:**3422–3423. http://dx.doi.org/10.1093/bioinformatics/bti553.
20. **Datsenko KA, Wanner BL.** 2000. One-step inactivation of chromosomal genes in Escherichia coli K-12 using PCR products. Proc Natl Acad Sci U S A **97:**6640–6645. http://dx.doi.org/10.1073/pnas.120163297.
21. **Charpentier X, Oswald E.** 2004. Identification of the secretion and translocation domain of the enteropathogenic and enterohemorrhagic Escherichia coli effector Cif, using TEM-1 beta-lactamase as a new fluorescence-based reporter. J Bacteriol **186:**5486–5495. http://dx.doi.org/10.1128/JB.186.16.5486-5495.2004.
22. **Moon AF, Mueller GA, Zhong X, Pedersen LC.** 2010. A synergistic approach to protein crystallization: combination of a fixed-arm carrier with surface entropy reduction. Protein Sci **19:**901–913. http://dx.doi.org/10.1002/pro.368.
23. **van Zon JS, Tzircotis G, Caron E, Howard M.** 2009. A mechanical

bottleneck explains the variation in cup growth during FcgammaR phagocytosis. Mol Syst Biol **5**:298. http://dx.doi.org/10.1038/msb.2009.59.
24. **Wang RF, Kushner SR.** 1991. Construction of versatile low-copy-number vectors for cloning, sequencing and gene expression in Escherichia coli. Gene **100**:195–199. http://dx.doi.org/10.1016/0378-1119(91)90366-J.
25. **Valdivia RH.** 1997. Fluorescence-based isolation of bacterial genes expressed within host cells. Science **277**:2007–2011. http://dx.doi.org/10.1126/science.277.5334.2007.
26. **Sathyabama S, Kaur G, Arora A, Verma S, Mubin N, Mayilraj S, Agrewala JN.** 2014. Genome sequencing, annotation and analysis of Salmonella enterica subspecies salamae strain DMA-1. Gut Pathog **6**:8. http://dx.doi.org/10.1186/1757-4749-6-8.
27. **Akeda Y, Galán JE.** 2005. Chaperone release and unfolding of substrates in type III secretion. Nature **437**:911–915. http://dx.doi.org/10.1038/nature03992.
28. **Frankel G, Phillips AD, Trabulsi LR, Knutton S, Dougan G, Matthews S.** 2001. Intimin and the host cell—is it bound to end in Tir(s)? Trends Microbiol **9**:214–218. http://dx.doi.org/10.1016/S0966-842X(01)02016-9.
29. **Wu H, Jones RM, Neish AS.** 2012. The Salmonella effector AvrA mediates bacterial intracellular survival during infection in vivo. Cell Microbiol **14**:28–39. http://dx.doi.org/10.1111/j.1462-5822.2011.01694.x.
30. **Pilar AVC, Reid-Yu SA, Cooper CA, Mulder DT, Coombes BK.** 2012. GogB is an anti-inflammatory effector that limits tissue damage during Salmonella infection through interaction with human FBXO22 and Skp1. PLoS Pathog **8**(6):e1002773. http://dx.doi.org/10.1371/journal.ppat.1002773.
31. **Rytkonen A, Poh J, Garmendia J, Boyle C, Thompson A, Liu M, Freemont P, Hinton JCD, Holden DW.** 2007. SseL, a Salmonella deubiquitinase required for macrophage killing and virulence. Proc Natl Acad Sci U S A **104**:3502–3507. http://dx.doi.org/10.1073/pnas.0610095104.
32. **Thomas SM, Brugge JS.** 1997. Cellular functions regulated by Src family kinases. Annu Rev Cell Dev Biol **13**:513–609. http://dx.doi.org/10.1146/annurev.cellbio.13.1.513.
33. **Trombert AN, Berrocal L, Fuentes JA, Mora GC.** 2010. S. Typhimurium sseJ gene decreases the S. Typhi cytotoxicity toward cultured epithelial cells. BMC Microbiol **10**:312. http://dx.doi.org/10.1186/1471-2180-10-312.
34. **Tsolis RM, Townsend SM, Miao EA, Miller SI, Ficht TA, Adams LG, Bäumler AJ.** 1999. Identification of a putative Salmonella enterica serotype typhimurium host range factor with homology to IpaH and YopM by signature-tagged mutagenesis. Infect Immun **67**:6385–6393.
35. **Newton HJ, Pearson JS, Badea L, Kelly M, Lucas M, Holloway G, Wagstaff KM, Dunstone MA, Sloan J, Whisstock JC, Kaper JB, Robins-Browne RM, Jans DA, Frankel G, Phillips AD, Coulson BS, Hartland EL.** 2010. The type III effectors NleE and NleB from enteropathogenic E. coli and OspZ from Shigella block nuclear translocation of NF-κB p65. PLoS Pathog **6**:e1000898. http://dx.doi.org/10.1371/journal.ppat.1000898.
36. **Rohde JR, Breitkreutz A, Chenal A, Sansonetti PJ, Parsot C.** 2007. Type III secretion effectors of the IpaH family are E3 ubiquitin ligases. Cell Host Microbe **1**:77–83. http://dx.doi.org/10.1016/j.chom.2007.02.002.
37. **Mirold S, Ehrbar K, Weissmüller A, Prager R, Tschäpe H, Rüssmann H, Hardt WD.** 2001. Salmonella host cell invasion emerged by acquisition of a mosaic of separate genetic elements, including Salmonella pathogenicity island 1 (SPI1), SPI5, and sopE2. J Bacteriol **183**:2348–2358. http://dx.doi.org/10.1128/JB.183.7.2348-2358.2001.
38. **Mallo GV, Espina M, Smith AC, Terebiznik MR, Alemán A, Finlay BB, Rameh LE, Grinstein S, Brumell JH.** 2008. SopB promotes phosphatidylinositol 3-phosphate formation on Salmonella vacuoles by recruiting Rab5 and Vps34. J Cell Biol **182**:741–752. http://dx.doi.org/10.1083/jcb.200804131.
39. **Knodler LA, Finlay B, Steele-Mortimer O.** 2005. The Salmonella effector protein SopB protects epithelial cells from apoptosis by sustained activation of Akt. J Biol Chem **280**:9058–9064. http://dx.doi.org/10.1074/jbc.M412588200.
40. **Cordero-Alba M, Ramos-Morales F.** 2014. Patterns of expression and translocation of the ubiquitin ligase SlrP in Salmonella enterica serovar Typhimurium. J Bacteriol **196**:3912–3922. http://dx.doi.org/10.1128/JB.02158-14.
41. **Ochman H, Wilson AC.** 1987. Evolution in bacteria: evidence for a universal substitution rate in cellular genomes. J Mol Evol **26**:74–86. http://dx.doi.org/10.1007/BF02111283.
42. **Ochman H, Groisman EA.** 1996. Distribution of pathogenicity islands in Salmonella spp. Infect Immun **64**:5410–5412.
43. **Katribe E, Bogomolnaya LM, Wingert H, Andrews-Polymenis H.** 2009. Subspecies IIIa and IIIb Salmonellae are defective for colonization of murine models of salmonellosis compared to Salmonella enterica subsp. I serovar typhimurium. J Bacteriol **191**:2843–2850. http://dx.doi.org/10.1128/JB.01223-08.
44. **Madsen M, Hangartner P, West K, Kelly P.** 1998. Recovery rates, serotypes, and antimicrobial susceptibility patterns of salmonellae isolated from cloacal swabs of wild Nile crocodiles (Crocodylus niloticus) in Zimbabwe. J Zoo Wildl Med **29**:31–34.
45. **Hansen-Wester I, Chakravortty D, Hensel M.** 2004. Functional transfer of Salmonella pathogenicity island 2 to Salmonella bongori and Escherichia coli. Infect Immun **72**:2879–2888. http://dx.doi.org/10.1128/IAI.72.5.2879-2888.2004.
46. **Wang Y, Li J, Hou S, Wang X, Li Y, Ren D, Chen S, Tang X, Zhou J-M.** 2010. A Pseudomonas syringae ADP-ribosyltransferase inhibits Arabidopsis mitogen-activated protein kinase kinases. Plant Cell **22**:2033–2044. http://dx.doi.org/10.1105/tpc.110.075697.
47. **Wilton M, Subramaniam R, Elmore J, Felsensteiner C, Coaker G, Desveaux D.** 2010. The type III effector HopF2Pto targets Arabidopsis RIN4 protein to promote Pseudomonas syringae virulence. Proc Natl Acad Sci U S A **107**:2349–2354. http://dx.doi.org/10.1073/pnas.0904739107.
48. **Lesnick ML, Reiner NE, Fierer J, Guiney DG.** 2001. The Salmonella spvB virulence gene encodes an enzyme that ADP-ribosylates actin and destabilizes the cytoskeleton of eukaryotic cells. Mol Microbiol **39**:1464–1470. http://dx.doi.org/10.1046/j.1365-2958.2001.02360.x.
49. **Simon NC, Aktories K, Barbieri JT.** 2014. Novel bacterial ADP-ribosylating toxins: structure and function. Nat Rev Microbiol **12**:599–611. http://dx.doi.org/10.1038/nrmicro3310.
50. **Barbieri JT, Sun J.** 2004. Pseudomonas aeruginosa ExoS and ExoT. Rev Physiol Biochem Pharmacol **152**:79–92.